


Better discrimination of the concomitant peri-ankle fractures in the spiral tibial shaft fractures by thin-slice axial and three-dimensional CT

Takashi Suzuki, MD, PhD^{a,b,*} , Taketo Kurozumi, MD, PhD^{a,b}, Yuhei Nakayama, MD^a, Kentaro Matsui, MD, PhD^a, Yoshinobu Watanabe, MD, PhD^a, Tetsuya Sakamoto, MD, PhD^b, Naoto Morimura, MD, PhD^b

Abstract

The objective of this study was to examine the morphologic features of spiral tibial shaft as well as concomitant fibular and peri-ankle fractures on multidetector high-resolution CT and to speculate about the mechanisms underlying these combined fractures.

This is a retrospective cohort study. A total of 197 tibial shaft fractures underwent multidetector high-resolution CT before intramedullary nailing. The presence and location of peri-ankle fractures were recorded using thin-slice axial CT. Tibial shaft fractures were classified as spiral or non-spiral. The morphologies of spiral tibial fractures and concomitant lateral malleolar fractures were delineated using three-dimensional CT.

Seventy-five spiral and 122 non-spiral fractures were identified. Peri-ankle fractures excluding lateral malleolar fractures were found in 77.3% of spiral fractures and 18.9% of non-spiral fractures. The most frequent location of peri-ankle fractures in the spiral group was the posterior malleolus, followed by the anterolateral distal tibia, while the medial malleolus was the most frequent site in the non-spiral group. Of 75 spiral fractures, 72 showed a fracture morphology attributed to external rotation force. There were 13 lateral malleolar fractures that were defined as within 6 cm from the distal end of the fibula. No lateral malleolar fractures showed the typical morphology of isolated supination/external rotation-type ankle injuries. The displaced syndesmotic injuries commonly coexisting in pronation/external rotation-type ankle injuries were not observed.

Most spiral tibial shaft fractures were caused by external rotation force. However, the morphology of concomitant peri-ankle fractures was inconsistent with typical mechanisms of isolated external rotation ankle injuries.

Abbreviations: 3D = three-dimensional, AO/OTA = Arbeitsgemeinschaft fuer Osteosynthesefragen/Orthopaedic Trauma Association, PER = pronation/external rotation, SER = supination/external rotation.

Keywords: ankle fracture, CT, external rotation, spiral fracture, tibial shaft fracture

Editor: Bo Liu.

The authors have no funding to disclose.

The authors have no conflicts of interest to disclose.

Ethical approval: This study was approved by the institutional review board of our hospital. Obtaining the informed consent from involved patients was waived by the institutional review board.

Data access: The datasets analyzed during the present study are available from the corresponding author on reasonable request.

The datasets generated during and/or analyzed during the present study are available from the corresponding author on reasonable request.

^aTrauma and Reconstruction Center, Teikyo University Hospital, Tokyo, Japan,

^bDepartment of Emergency Medicine, Teikyo University, Tokyo, Japan.

* Correspondence: Takashi Suzuki, Trauma and Reconstruction Center, Teikyo University Hospital, 2-11-1 Kaga, Itabashi-ku, Tokyo 173-8606, Japan (e-mail: takashisuzuki911@yahoo.co.jp).

Copyright © 2021 the Author(s). Published by Wolters Kluwer Health, Inc. This is an open access article distributed under the terms of the Creative Commons Attribution-Non Commercial License 4.0 (CCBY-NC), where it is permissible to download, share, remix, transform, and buildup the work provided it is properly cited. The work cannot be used commercially without permission from the journal.

How to cite this article: Suzuki T, Kurozumi T, Nakayama Y, Matsui K, Watanabe Y, Sakamoto T, Morimura N. Better discrimination of the concomitant peri-ankle fractures in the spiral tibial shaft fractures by thin-slice axial and three-dimensional CT. *Medicine* 2021;100:40(e27429).

Received: 2 May 2021 / Received in final form: 20 August 2021 / Accepted: 14 September 2021

<http://dx.doi.org/10.1097/MD.0000000000027429>

1. Introduction

Fractures of the tibial shaft are relatively common among adult trauma patients.^[1] Of the several basic fracture patterns, the spiral morphology comprises one-quarter to fully half, which is mainly due to low-energy trauma.^[1–3] Previously, ankle joint injuries were known to occasionally occur in association with tibial shaft fractures, especially with the spiral pattern.^[2,4–8] Over the past decade, with the increased use of CT, the association of ankle fracture with tibial shaft fracture has been well investigated.^[2,4–21] The morphology of spiral tibial shaft fractures has been thought to correspond well with the torsional force, which could frequently cause posterior malleolar fractures.^[2,4,7,19–21] Involvement of an ankle component has been automatically correlated to analogous torsional mechanisms of either supination/external rotation (SER)- or pronation/external rotation (PER)-type fractures in the Lauge–Hansen classification.^[2,4,7,8,22] However, the actual mechanisms underlying combined fractures have not been well explained and remain under discussion.^[8,11,14,18,21]

Despite increasing awareness of the possibility of ankle fracture concomitant with spiral tibial shaft fracture, the three-dimensional (3D) morphology of spiral fracture patterns of the tibia has received little attention in the literature.^[5,9,11] Morphological correlations between tibial shaft fractures and fibular or peri-ankle fractures may facilitate an understanding of the mechanisms underlying such combined fractures.

The primary objective of this study was to determine the exact force causing spiral tibial shaft fractures by delineating the fracture morphology. The secondary objective was to identify the locations of both fibular and peri-ankle fractures, to clarify correlations with tibial shaft fractures. We aimed to provide speculations regarding whether the mechanisms of typical isolated ankle injuries could account for spiral tibial shaft fractures and associated injuries.

2. Patients and methods

This retrospective cohort study was approved by the institutional review board (ethics proposal number: TUI-COI 19-174). We performed a review of operation registries at a level-1 academic trauma center between January 2010 and December 2019. Patients who underwent intramedullary nailing of a tibial shaft fracture were identified and included in this study. Tibial shaft fractures were divided into spiral and non-spiral groups based on 3D surface rendering reconstruction images and the Arbeitsgemeinschaft fuer Osteosynthesefragen / Orthopaedic Trauma Association (AO/OTA) classification.^[23]

During the 10-year study period, 257 tibial shaft fractures were treated by intramedullary nailing at our institution. Of these, 42 patients did not undergo preoperative CT for assessment of tibial shaft fractures due to the general condition of the patient or a lack of available time before emergent operations, particularly during the early study period. Thin-slice volume data from CT were not stored in Picture Archiving and Communication Systems as of this study in 18 patients. Thus, CT data for 197 tibial shaft fractures were included in this study. Patients comprised 145 men and 46 women, of whom 6 patients had undergone intramedullary nailing for bilateral tibial shaft fractures.

Radiographic images were reviewed and interpreted using Picture Archiving and Communication Systems software (Centricity Enterprise Web v3.0 Internet Explorer; GE Healthcare, Little Chalfont, UK) through a 19-inch Liquid Crystal Display monitor, with a standardized aspect ratio of 5:4, resolution of 1280 × 1024 pixels. All CT images were obtained using a 64- or 320- row multidetector CT scanner (Aquilion 64 or 320; 50 mA, 120 kV, or Toshiba Medical Systems, Otawara, Japan). Two fellowship-trained orthopedic trauma surgeons (TaS and YN) reviewed the 3D surface rendering reconstruction images and thin-slice axial volume data (0.5 mm slice thickness) images independently. We assumed the fracture pattern with inter-reviewer agreement. When disagreement occurred, the final decision was made with the additional information from the two-dimensional reformatted images in the sagittal and coronal planes.

2.1. Morphology of tibial shaft fracture

To define spiral fractures of the tibia, images from 3D-CT were reviewed and rotated at various angles using Picture Archiving and Communication Systems software. Spiral fracture was confirmed if the fracture plane was oblique and encircled the long axis of the tibia in conjunction with a vertical fracture line connecting the proximal and distal ends of the oblique fracture line.^[24] The tibial shaft is triangular in cross-section and forms three surfaces: medial, lateral, and posterior. Thus, the fracture morphology of spiral patterns was delineated on each surface of the tibial shaft. The location of the vertical fracture line on one of the three surfaces, and the course of lines as medial to lateral, proximal to distal, or posterior to anterior were also recorded.

2.2. Morphology of peri-ankle fracture

Presence and location of peri-ankle fractures on thin-slice axial CT images were recorded. The fracture line was reviewed as 0.5 mm thickness slice axial CT images using window level: 500 and window width: 2300 as a standard contrast. The presence of fracture was confirmed if more than two axial slices showed fracture lines. Lateral malleolar fractures were excluded from the number of peri-ankle fractures and investigated separately. Syndesmotic injuries were identified 1 cm above the joint space on axial CT images according to two previously reported criteria including tibio-fibular diastasis and translation of the fibula in the incisura,^[25,26] and were also recorded.

2.3. Morphology of fibular fracture

Five categories were established in terms of relative location to the tibial shaft fractures: distal, same, proximal, segmental, and absent. We defined the location of the fibular fracture as the same level if it was located ≤ 5 cm proximal or distal to the center of the tibial shaft fracture. In addition, lateral malleolar fracture was defined within 6 cm from the distal end of the fibula, which almost corresponded to AO/OTA 4F3. The fracture morphology of lateral malleolar fractures was evaluated and compared with typical lateral malleolus fractures on 3D-CT.^[27,28]

2.4. Statistical analyses

Statistical analyses included comparisons between spiral and non-spiral groups. Fisher's exact test or the chi-square test was used to compare categorical data between groups. Mean \pm standard deviation was used for continuous variables. IBM SPSS Statistics version 24.0 (IBM Corp., Armonk, NY, USA) was used for all statistical analyses. Values of $P < .05$ were defined as significant.

3. Results

3.1. Tibial shaft fracture

According to the AO/OTA classification, there were 92 type A, 79 type B, and 26 type C fractures, consisting of 75 spiral fractures and 122 non-spiral fractures. The spiral group included 46 type A1, 28 type B2, and one type C2 fractures (Fig. 1).

The center of tibial shaft fractures was located on the proximal half in 22 cases and on the distal half in 165 cases. In the

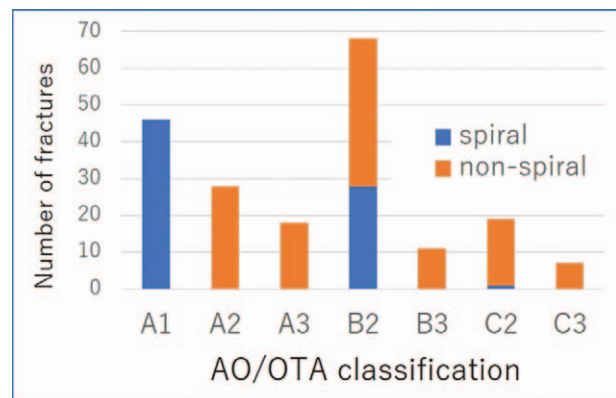


Figure 1. Fracture type distribution according to AO/OTA classification.

Table 1**Univariate analysis for categorical variables.**

		All fractures (n = 197)	Spiral fractures (n = 75)		Non-spiral fractures (n = 122)		P value
Side	Right	109	50	(66.7%)	59	(48.4%)	.012*
	Left	88	25	(33.3%)	63	(51.6%)	
Location of tibial fracture	Proximal half	22	3	(4.0%)	19	(15.6%)	<.001*
	Distal half	165	71	(94.7%)	94	(77.0%)	
	Combined	10	1	(1.3%)	9	(7.4%)	
Location of fibular fracture relative to tibial fracture	Proximal	55	42	(56.0%)	13	(10.7%)	<.001*
	Same	69	9	(12.0%)	60	(49.2%)	
	Distal	28	15	(20.0%)	13	(10.7%)	
	Segmental	28	5	(6.7%)	23	(18.9%)	
	None	17	4	(5.3%)	13	(10.7%)	
Overall peri-ankle fracture	Presence	81	58	(77.3%)	23	(18.9%)	<.001*
	Absence	116	17	(22.7%)	99	(81.1%)	
Presence of posterior malleolar fracture	Presence	57	48	(64.0%)	9	(7.4%)	<.001*
	Absence	140	27	(36.0%)	113	(92.6%)	
Open fracture	Presence	117	33	(44.0%)	84	(68.9%)	.001*
	Absence	80	42	(56.0%)	38	(31.1%)	

Values are total number (percentage in the same column).

*Fisher's exact test or chi-square test was significant at $P < .05$.

remaining 10 fractures, the location was difficult to determine due to either segmental or comminuted fractures in type C. The comparison between spiral and non-spiral fractures is shown in Table 1. Spiral fractures had a lower incidence of open fracture, and tended to occur in the distal half of the tibia more frequently compared to non-spiral fractures.

The morphology of spiral patterns showed specific features. In all cases, the longitudinal split of the spiral fracture, shown as a roughly vertical line relative to the axis of the tibia, was located mainly on the posterior surface of the tibial shaft. This means that the first failure of bone constantly occurred on the anterior side of the tibia under tension force.^[24] In 72 of 75 cases, the oblique fracture line ran from medial-distal to lateral-proximal (Fig. 2). This is shown on plain anteroposterior radiographs in which the distal fracture fragment beak exists relatively laterally. In contrast, only three cases showed fractures in the contra-direction (Fig. 3).

3.2. Peri-ankle fracture

The overall prevalence of concomitant peri-ankle fractures was 41.1% (81/197). Spiral tibial shaft fractures showed a significantly higher incidence of concomitant peri-ankle fractures. In 58 of 75 (77.3%) spiral tibial fractures, a total of 67 peri-ankle fractures were identified. The most frequent location of concomitant peri-ankle fracture was the posterior malleolus. In addition, an intra-articular fragment of the anterolateral distal tibia (Tillaux–Chaput type) was appearing in 12 of 75 tibial fractures on thin-slice axial CT (Table 2). Combined posterior malleolar and Tillaux–Chaput-type fractures were seen in six cases (Fig. 4). In contrast, the combination of posterior malleolar and medial malleolar fractures was seen only in one case. In the non-spiral group, a total of 27 peri-ankle fractures were seen in

23 of the 122 (18.9%) tibial shaft fractures. The most frequent fracture site was the medial malleolus, followed by the posterior malleolus (Table 2).

3.3. Fibular fracture

In all tibial shaft fractures, the level of fibular fracture relative to the tibial shaft fracture was proximal in 55 cases, the same in 69, distal in 28, and absent in 17. The remaining 28 fractures were segmental and the relative location was thus difficult to determine. Fibular fractures were located at the same level less

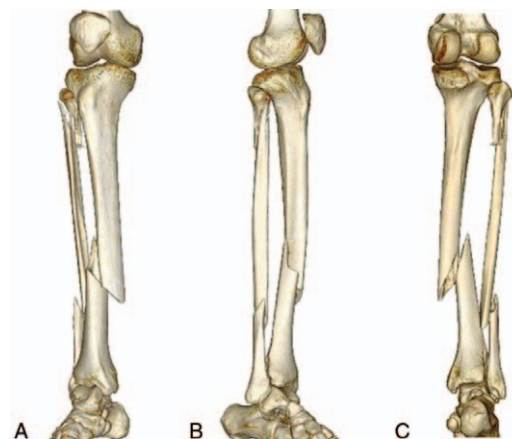


Figure 2. A 37-year-old male who sustained spiral tibial shaft fracture showing external rotation force. (A) Medial surface, (B) lateral surface, (C) posterior surface of the leg on 3D-CT. An oblique fracture line runs antero-proximal to postero-distal on the medial surface, postero-proximal to antero-distal on the lateral surface. A vertical fracture line exists on the posterior surface.

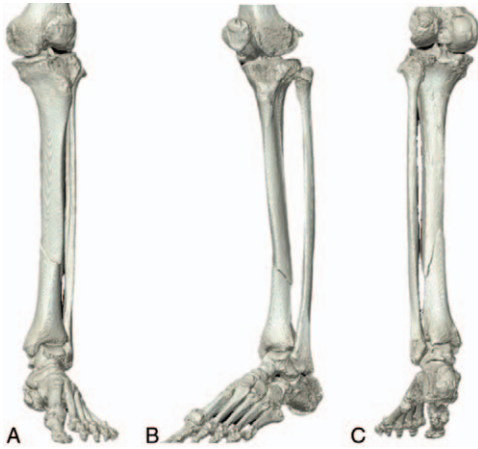


Figure 3. A 52-year-old female who sustained spiral tibial shaft fracture showing internal rotation force. (A) Medial surface, (B) lateral surface, (C) posterior surface of the leg on 3D-CT. An oblique fracture line runs postero-proximal to antero-distal on the medial surface, antero-proximal to postero-distal on the lateral surface. A vertical fracture line exists on the posterior surface.

frequently in the spiral group, and with proximal in 56%, followed by distal in 20%. In the non-spiral group, the level of fibular fracture was the same in 49.2%, followed by segmental in 18.9% (Table 1).

Lateral malleolar fracture was seen in 13 cases (17.3%) in the spiral group and 19 cases (15.6%) in the non-spiral group. In the spiral group, 10 of the 13 cases showed short spiral patterns, in which the main fracture line ran obliquely from posterolateral to anteromedial on the lateral malleolus (Table 3). Eight of these 10 cases displayed a similar course to SER-type ankle injuries that showed spiral extension into the anterior syndesmosis. However, all eight cases exhibited wedge or multiple fragments corresponding to AO/OTA 4F3B, and no lateral malleolar fractures showed typical SER-type ankle injuries. No evidence of syndesmotic injury was identified in the spiral group, whereas fibular malposition in the incisura was identified in two cases in the non-spiral group.

4. Discussion

To the best of our knowledge, this is the first study to evaluate the morphological characteristics of spiral tibial shaft fractures and concomitant lateral malleolar fractures using 3D-CT. Moreover,

Table 2
Variation of peri-ankle fractures associated with tibial shaft fractures.

	Spiral n = 67	Non-spiral n = 27
Posterior malleolus	48	9
Tillaux-Chaput	12	5
Medial malleolus	4	11
Wagstaffe-Le Fort	2	0
Avulsion of PITFL (fibular side)	1	0
Anterior rim of distal tibial plafond	0	2

Fibular fractures consisted of lateral malleolus was excluded.
PITFL = posterior inferior tibiofibular ligament.

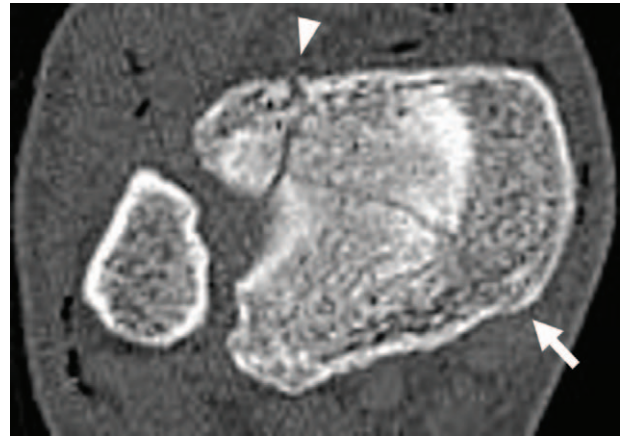


Figure 4. A 44-year-old male sustained spiral tibial shaft fracture. The axial CT image showed combination of posterior malleolar (arrow) and Tillaux-Chaput type (arrow head) fractures.

the current study meticulously investigated concomitant peri-ankle fracture on thin-slice axial CT images. These revealed that the fracture line of the tibia ran from medial-distal to lateral-proximal in most cases, and the vertical fracture line was constantly identified on the posterior surface of the tibial shaft. The morphology of concomitant lateral malleolar fracture, when present, was not the same as SER-type ankle injuries. With regard to peri-ankle fractures, not only posterior malleolar fractures, but also other types of peri-ankle fractures could often be present concomitantly.

Biomechanically, when torsional force is applied to a long bone, failure occurs first on the side under tension, resulting in a spiral fracture inclined 45° with respect to the long-bone axis. Finally, the torsional force creates a longitudinal split on the side under compression.^[24] Some authors have reported that in most spiral tibial fractures, the inferior apex of the spiral was medial, extending superiorly to a posterolateral apex on plain radiographs.^[5,9,11,16] This fracture line is well explained biomechanically by external rotation force to the ankle.^[24] In the present study, most spiral fractures were attributed to external rotation force, and internal rotation force was infrequent. On the other hand, the constant presence of the vertical fracture line on the posterior surface indicated eccentric torsional force producing tension on the anterior side. This could be explained as spiral fractures resulting from torsional force under the existence of posteriorly deviated axial loading.

In the present study, the prevalence of overall concomitant peri-ankle fractures was 41.1% and more frequent than in previous studies, in which rates of ankle fracture have been

Table 3
Fracture type of lateral malleolus.

	Spiral n = 13	Non-spiral n = 19
Spiral	10	2
Oblique	1	5
Transverse	1	6
Comminuted	0	5
Segmental	1	1

reported as 0.9–2.5%.^[2,5,6,8,12,15,20] As previously reported,^[6–21] posterior malleolar fractures were frequently associated with spiral tibial shaft fractures. Tillaux–Chaput-type fractures were the second most common, as described in a few reports.^[10,12,19] Further, the combination of posterior malleolar and Tillaux–Chaput-type fractures was identified in six spiral tibial shaft fractures. These combined fractures may occur with torsional force, as Warner et al reported that anterior inferior tibiofibular ligament injury or Tillaux–Chaput fracture could coexist with posterior malleolar fractures in spiral tibial fractures.^[13] Similarly, Kellam et al reported that posterior malleolar fractures associated with tibial shaft fractures often exhibited an additional fracture line oriented in the sagittal plane, resulting in an anterolateral fragment.^[21] The combination of posterior malleolar and Tillaux–Chaput-type fractures may be a common characteristic in spiral tibial shaft fractures.

Typically, torsional force to the leg results in a fracture pattern in which the tibia and fibula are fractured at different levels.^[2,4,5,9] In the current study, only 12% of spiral tibial fractures showed fibular fractures at the same level, whereas 49.2% of non-spiral fractures had fibular fractures at the same level. Since spiral tibial fracture usually occurs in the infra-isthmal part of the diaphysis, relatively proximal fibular fractures are far more common.^[2,7,11,14,15,17,20] Some authors have suggested that concomitant posterior malleolar fractures are part of typical ankle injuries and proximal fibular fractures indicate rupture of an interosseous membrane such as PER-type ankle injuries or Maisonneuve injuries.^[2,8] Theoretically, displaced syndesmotic injuries should coexist when displaced fibular fractures are caused by PER-type ankle injuries. In addition, medial-side injuries including medial malleolar fractures or deltoid ligament injuries must be present in PER-type ankle injuries. In the current study, no signs of syndesmotic injuries were observed. Although the current study did not evaluate deltoid ligament injuries, only one combination of posterior and medial malleolar fractures was apparent.

In the light of the pathoanatomy of these combined tibial and posterior malleolar fractures, several reports have described the most frequent mechanism as indirect twisting with external rotation of the supinated or pronated ankle since stage 3 and 4 SER-type ankle injuries and stage 4 PER-type ankle injuries include posterior malleolar fractures.^[2,4,7,8,22] However, the morphology of lateral malleolar fractures on 3D-CT was not the same as that of SER-type ankle injuries, due to its wedge or multifragmentary nature. Moreover, it has been reported that the morphology of posterior malleolar fractures associated with spiral tibial shaft fractures differed from that of isolated ankle injuries in terms of location, shape, and size.^[19–21] Judging from the evidence that most posterior malleolar fractures are non-displaced or incomplete in spiral tibial shaft fractures, these combined fractures seem not to represent simple extension of isolated ankle injuries and can be considered as different clinical entities.^[11,14,20] To correlate with the posterior vertical fracture line of the tibia, which must be on the compression side, it may be reasonable to expect that external rotation force was applied with the knee flexed and ankle dorsiflexed, in which the load bearing axis passed through the posterior of the tibia. This speculation is strongly supported by the fact that spiral tibial shaft fractures are the most common tibial fractures in skiers, for whom the ankles and feet are locked in the ski boot.^[29,30]

Several limitations to this study must be clarified. First, the retrospective nature of the study meant that consecutive patients

were unable to be included. Second, we tried to determine fracture morphology not only for the lateral malleolus, but also for the middle and proximal fibula. However, reliably differentiating between oblique and spiral fractures, or bending wedge and spiral wedge fractures, was not possible, since those locations are thin and small. Third, atypical and transitional fracture patterns are always a possibility. Within our strict definition of spiral fracture, we may have classified some fractures caused by torsional force to the non-spiral group. Fourth, normal measurements of the tibio-fibular joint did not preclude syndesmotic injuries.^[31] Since no dynamic stress test was applied to the ankle joint after intramedullary nailing, underdiagnosed syndesmotic injuries may have existed in some cases. Finally, the injury mechanism was speculated on the basis of radiographic findings, and was not confirmed from cadaveric investigations. Further studies evaluating this hypothesis should be performed in cadaver models by monitoring forces delivered to the dorsiflexed ankle joint.

5. Conclusions

The overall prevalence of concomitant peri-ankle fractures on thin-slice CT images was higher than previously reported. External rotation force caused the combination of spiral tibial shaft and peri-ankle fractures. However, the morphology of concomitant peri-ankle fractures was inconsistent with typical mechanisms of isolated external rotation ankle injuries. The exact mechanisms behind these combined fractures should be distinguished from the entity of isolated external rotation ankle injuries.

Author contributions

Conceptualization: Takashi Suzuki, Yuhei Nakayama.

Data curation: Taketo Kurozumi, Kentaro Matsui.

Formal analysis: Yoshinobu Watanabe.

Investigation: Takashi Suzuki, Yuhei Nakayama.

Methodology: Yoshinobu Watanabe.

Project administration: Naoto Morimura.

Supervision: Tetsuya Sakamoto, Naoto Morimura.

Writing – original draft: Takashi Suzuki.

Writing – review & editing: Taketo Kurozumi.

References

- [1] Boulton CL, O'Toole RV, Tornetta PIII, Ricci WM, Ostrum RF, McQueen MM, McKee MD, Court-Brown CM. Tibia and fibula shaft fractures. Rockwood and Green's fractures in adults 9th ed. Philadelphia: Wolters Kluwer; 2020;2687–751.
- [2] Böstman OM. Displaced malleolar fractures associated with spiral fractures of the tibial shaft. *Clin Orthop Relat Res* 1988;228:202–7.
- [3] Larsen P, Elsoe R, Hansen SH, Graven-Nielsen T, Laessoe U, Rasmussen S. Incidence and epidemiology of tibial shaft fractures. *Injury* 2015;46:746–50.
- [4] Lonner JH, Jupiter JB, Healy WL. Ipsilateral tibia and ankle fractures. *J Orthop Trauma* 1993;7:130–7.
- [5] Robinson CM, McLauchlan GJ, McLean IP, Court-Brown CM. Distal metaphyseal fractures of the tibia with minimal involvement of the ankle. Classification and treatment by locked intramedullary nailing. *J Bone Joint Surg Br* 1995;77:781–7.
- [6] Kukkonen J, Heikkilä JT, Kyyrönen T, Mattila K, Gullichsen E. Posterior malleolar fracture is often associated with spiral tibial diaphyseal fracture: a retrospective study. *J Trauma* 2006;60:1058–60.
- [7] Boraiah S, Gardner MJ, Helfert DL, Lorich DG. High association of posterior malleolus fractures with spiral distal tibial fractures. *Clin Orthop Relat Res* 2008;466:1692–8.

- [8] Stuermer EK, Stuermer KM. Tibial shaft fracture and ankle joint injury. *J Orthop Trauma* 2008;22:107–12.
- [9] Hou Z, Zhang Q, Zhang Y, Li S, Pan J, Wu H. A occult and regular combination injury: the posterior malleolar fracture associated with spiral tibial shaft fracture. *J Trauma* 2009;66:1385–90.
- [10] Purnell GJ, Glass ER, Altman DT, Sciulli RL, Muffly MT, Altman GT. Results of a computed tomography protocol evaluating distal third tibial shaft fractures to assess noncontiguous malleolar fractures. *J Trauma* 2011;71:163–8.
- [11] Hou Z, Zhang L, Zhang Q, et al. The “communication line” suggests occult posterior malleolar fracture associated with a spiral tibial shaft fracture. *Eur J Radiol* 2012;81:594–7.
- [12] Schottel PC, Berkes MB, Little MT, et al. Predictive radiographic markers for concomitant ipsilateral ankle injuries in tibial shaft fractures. *J Orthop Trauma* 2014;28:103–7.
- [13] Warner SJ, Schottel PC, Garner MR, Helfet DL, Lorich DG. Ankle injuries in distal tibial spiral shaft fractures: results from an institutional change in imaging protocol. *Arch Orthop Trauma Surg* 2014;134:1661–6.
- [14] Tsai CE, Su YP, Feng CK, Chen CM, Chiu FY, Liu CL. Concomitant tibial shaft and posterior malleolar fractures can be readily diagnosed from plain radiographs: a retrospective study. *J Chin Med Assoc* 2014;77:95–100.
- [15] Kempegowda H, Maniar HH, Richard R, et al. Posterior malleolar fractures associated with tibial shaft fractures and sequence of fixation. *J Orthop Trauma* 2016;30:568–71.
- [16] Marchand LS, Rane AA, Working ZM, et al. Radiographic investigation of the distal extension of fractures into the articular surface of the tibia (The RIDEFAST study). *J Orthop Trauma* 2017;31:668–74.
- [17] Sobol GL, Shaath MK, Reilly MC, Adams MR, Sirkin MS. The incidence of posterior malleolar involvement in distal spiral tibia fractures: is it higher than we think? *J Orthop Trauma* 2018;32:543–7.
- [18] Huang Z, Liu Y, Xie W, Li X, Qin X, Hu J. Pre-operative radiographic findings predicting concomitant posterior malleolar fractures in tibial shaft fractures: a comparative retrospective study. *BMC Musculoskelet Disord* 2018;19:86.
- [19] Mitchell PM, Harms KA, Lee AK, Collinge CA. Morphology of the posterior malleolar fracture associated with a spiral distal tibia fracture. *J Orthop Trauma* 2019;33:185–8.
- [20] Hendrickx LAM, Cain ME, Sierevelt IN, et al. Incidence, predictors, and fracture mapping of (occult) posterior malleolar fractures associated with tibial shaft fractures. *J Orthop Trauma* 2019;33:e452–8.
- [21] Kellam PJ, Haller JM, Rothberg DL, Higgins TF, Marchand LS. Posterior malleolar fracture morphology in tibial shaft versus rotational ankle fractures: the significance of the computed tomography scan. *J Orthop Trauma* 2019;33:e459–65.
- [22] Lauge-Hansen N. Fractures of the ankle. II. Combined experimental-surgical and experimental-roentgenologic investigations. *Arch Surg* 1950;60:957–85.
- [23] Meinberg EG, Agel J, Roberts CS, Karam MD, Kellam JF. Fracture and dislocation classification compendium-2018. *J Orthop Trauma* 2018;32: S1–170.
- [24] Bottlang M, Fitzpatrick DC, Claes L, Anderson DD, Tornetta PIII, Ricci WM, Ostrum RF, McQueen MM, McKee MD, Court-Brown CM. Biomechanics of fractures and fracture fixation. *Rockwood and Green's Fractures in adults 9th ed.* Philadelphia: Wolters Kluwer; 2020;1–42.
- [25] Gifford PB, Lutz M. The tibiofibular line: an anatomical feature to diagnose syndesmosis malposition. *Foot Ankle Int* 2014;35:1181–6.
- [26] Lepojärvi S, Pakarinen H, Savola O, Haapea M, Sequeiros RB, Niinimäki J. Posterior translation of the fibula may indicate malreduction: CT study of normal variation in uninjured ankles. *J Orthop Trauma* 2014;28:205–9.
- [27] Choi Y, Kwon SS, Chung CY, Park MS, Lee SY, Lee KM. Preoperative radiographic and CT findings predicting syndesmotic injuries in supination-external rotation-type ankle fractures. *J Bone Joint Surg Am* 2014;96:1161–7.
- [28] Chun DI, Kim J, Kim YS, et al. Relationship between fracture morphology of lateral malleolus and syndesmotic stability after supination-external rotation type ankle fractures. *Injury* 2019;50:1382–7.
- [29] Deibert MC, Aronsson DD, Johnson RJ, Ettliger CF, Shealy JE. Skiing injuries in children, adolescents, and adults. *J Bone Joint Surg Am* 1998;80:25–32.
- [30] Stenroos A, Pakarinen H, Jalkanen J, Mälkiä T, Handolin L. Tibial fractures in alpine skiing and snowboarding in Finland: a retrospective study on fracture types and injury mechanisms in 363 patients. *Scand J Surg* 2016;105:191–6.
- [31] Bartončiček J, Rammelt S, Kašper Š, Malík J, Tuček M. Pathoanatomy of Maisonneuve fracture based on radiologic and CT examination. *Arch Orthop Trauma Surg* 2019;139:497–506.